Biobreeding

SCIEPublish

Article

Integrated Multi-Omics and Biochemical Analyses Elucidate Salinity Stress-Related Physiological Responses in Skeletal Muscle of *Ictalurus punctatus*

Yongqiang Duan [1], Luyu Tang [1,2], Hongyan Liu [1,3], Minghua Wang [1,3], Liqiang Zhong [1,3], Ju Liu [1], Xiaohui Chen [1,2,3] and Shiyong Zhang [1,2,3,*]

[1] National Genetic Breeding Center of Channel Catfish, Freshwater Fisheries Research Institute of Jiangsu Province, Nanjing 210017, China; yqduan0712@163.com (Y.D.); dyq970712@163.com (L.T.); njsfdxliuhongyan@163.com (H.L.); wangminghua18@sina.com (M.W.); lqzhongffri@hotmail.com (L.Z.); juliuffrijs@sina.com (J.L.); cxiaohui416@hotmail.com (X.C.)

[2] College of Marine Science and Fisheries, Jiangsu Ocean University, Lianyungang 222005, China

[3] The Jiangsu Provincial Platform for Conservation and Utilization of Agricultural Germplasm, Nanjing 210014, China

* Corresponding author. E-mail: shiyongzhang@hotmail.com (S.Z.)

Received: 10 September 2026; Revised: 19 October 2026; Accepted: 26 October 2026; Available online: 18 November 2026

ABSTRACT: Freshwater resources have been declining in recent years, and the amount of acreage available for freshwater aquaculture has significantly decreased. The increasing need for freshwater aquaculture has led to the development of saline alkali aquaculture as a significant solution. The molecular adaption mechanism of the channel catfish's reaction to salinity stress is further clarified by performing multiomics correlation analysis and biochemical detection of fatty acids and mineral elements in the muscle tissue. Our research shows that salt stress significantly affects catfish lipid metabolism, oxidative stress, osmotic homeostasis, and partial immune response. Fatty acid synthesis, decomposition, and extension, branched chain amino acid decomposition, and other pathways that are influenced by high and low salt stress have a lot in common, according to Kyoto Encyclopedia of Genes and Genomes (KEGG) pathway enrichment research and Gene Ontology (GO) function annotation. Trend analysis results indicated that both high and low salt had an impact on the body's osmotic homeostasis simultaneously, that metabolic disorders and imbalances in energy utilization were only observed in the high salt group, and that the majority of trend-enriched genes did not significantly differ between the low salt group and the control group. The findings above are essentially in line with the mineral element and fatty acid detection results. The variations in osmotic balance and energy use of fish fry in the salinity group are also indirectly supported by the high expression of Na^+, K^+, Mg^{2+}, and Se elements. The de-stress test demonstrated that the large-scale damage was reversible and far less than that of the preceding stage. The steady-state control mechanism of channel catfish under salinity stress may be revealed thanks to these studies, which also offer insight into how drastic salinity fluctuations affect channel catfish in aquaculture practices.

Keywords: Salinity stress; Channel catfish; Metabolomics; Proteomics; Multi-omics analysis

© 2026 The authors. This is an open access article under the Creative Commons Attribution 4.0 International License (https://creativecommons.org/licenses/by/4.0/).

1. Introduction

Salinity is a critical abiotic environmental factor that profoundly influences the physiological functions of aquatic organisms [1]. Fluctuating salinity levels represent a prevalent environmental stressor in aquaculture, significantly impairing developmental processes, survival rates, metabolic operations, immune responses, and other physiological activities in aquatic species [2,3]. Excessive salt stress disrupts hydro-mineral balance and compromises osmotic homeostasis. To adapt to salinity variations, aquatic organisms must regulate ion transporter activity and modulate the expression of osmoregulation-related genes to maintain internal environmental stability [4]. Furthermore, salt stress induces oxidative damage through the accumulation of free radicals and reactive oxygen species, causing detrimental effects on essential cellular components including proteins, nucleic acids, and membrane structures. This oxidative challenge activates the organism's antioxidant defense mechanisms to enhance resistance to oxidative injury [5,6]. Additionally, salt stress can disrupt endocrine hormone secretion, create imbalances in energy and material metabolism, and adversely affect immune competence [7,8].

The channel catfish (*Ictalurus punctatus*), classified within the Siluriformes order and Ictaluridae family, represents a globally significant aquaculture species introduced to China during the 1980s [9]. This species exhibits stage-dependent salinity tolerance throughout its development. With annual production exceeding 375,000 tons in China, it holds substantial commercial importance in freshwater aquaculture due to its remarkable environmental adaptability and superior meat quality [10]. Major production regions include Guangdong, Jiangsu, Henan, and Hubei provinces, with Jiangsu's coastal tidal areas comprising over 10,000 hectares of cultivation zones [11]. Industrial-scale farming has also expanded to inland saline-alkaline regions, including low-lying areas along the Yellow River in Henan and Shaanxi provinces, Ningxia Autonomous Region, and the saline-alkaline plateau in Xinjiang [12].

Salinity tolerance thresholds vary across developmental stages: fertilized eggs tolerate 16 practical salinity units (psu), hatching stages 6 psu, yolk-sac larvae 10 psu, juvenile phases 8–9 psu, and adult fish (150 days post-hatch) withstand maximum salinities of 10–12 psu [13,14]. Although previous investigations indicated limited salt tolerance in this species [15,16], our preliminary research demonstrated that channel catfish fry reared in low-salinity conditions achieved growth performance and survival rates comparable to freshwater cultivation [17]. To elucidate the molecular mechanisms underlying salt stress adaptation, we employed proteomic and metabolomic approaches to analyze muscle tissue responses. Investigation of differentially expressed proteins and metabolites revealed key molecular pathways involved in salt stress response. Concurrently, desalination stress experiments monitored growth performance and survival rates in juvenile fish. These findings provide valuable insights for commercial aquaculture practices and establish a foundation for understanding homeostatic regulatory mechanisms in channel catfish under saline stress conditions.

The remainder of this manuscript is organized as follows. Section 2 (Materials and Methods) details the experimental design, salinity challenge protocol, fatty acid and mineral element detection, and the metabolomic, proteomic, trend, and integrative analytical pipelines. Section 3 (Results) presents changes in biochemical parameters; metabolomic profiling, including multivariate statistics and differential enrichment; proteomic profiling, including GO/KEGG enrichment and trend analysis; and multi-omics integration. Section 4 (Discussion) interprets the molecular mechanisms underlying salinity stress responses across the omics and biochemical levels. Section 5 (Conclusions) summarizes the key findings, acknowledges study limitations, and outlines implications for channel catfish aquaculture in saline-alkaline waters.

2. Materials and Methods

2.1. Ethics Statement

All experiments were performed in accordance with the Regulations of the Animal Ethics Committee and were approved by the Institutional Review Board on Bioethics and Biosafety of Freshwater Fisheries Research Institute of Jiangsu Province (No. FT, 22003).

2.2. Salinity Challenge Experiment and Fish Sampling

Channel catfish fries were obtained from the National Genetics & Breeding Center of Channel Catfish (Nanjing, Jiangsu Province, China). A total of 1000 fries with a body weight of 20–30 g were reared in commercial fish ponds (5 m × 5 m × 1 m) for 7 days before the experiment, under controlled conditions (20 ± 0.5 °C; 14:10 h light/dark cycle; oxygen content 5.7 ± 0.4 mg·L^{-1}). Individuals were randomly divided into nine experimental tanks (2 m × 2 m × 1 m, N = 20 in each tank) and acclimatized in freshwater for 7 days before the salinity trial. These experimental tanks were equally divided into three groups, including a control group (C group) and 5.0 (L group), 9.0 psu (H group) salinity groups. Tanks contained fry of similar average body weight (27.72 ± 0.84 g). Three biological replicates were performed for each group. Salinity was increased by 1 psu/day over 9 days toward the target ppt. Salinities were maintained by pre-mixing seawater and distilled water, with water changes performed daily. Water temperature varied over the course of exposures (between 25.6–28.9 °C), but was consistent across all tanks (26.3 ± 0.67 °C). Equal quantities of Fish Diet (Cargill, Zhenjiang, China) were provided to each tank daily. Following an 8-week period of salt stress, the salinity began to decline toward freshwater on the 9th week, dropping by 1 psu each day. Week 9 marked the beginning of the stress reduction trial, which concluded at week 16. Every two weeks throughout the duration of the trial, each group's weight was measured and documented.

During sampling, experimental catfish were humanely anesthetized with 0.1% tricaine methanesulfonate (MS-222) (Sigma-Aldrich, Saint Louis, MO, USA), and muscle from three individuals/tank was dissected, immediately frozen in liquid nitrogen, and stored at −80 °C for omics and antioxidant enzyme activity analyses. This study is not a clinical trial and is not suitable for submitting the necessary registration details.

2.3. Muscle Fatty Acid and Mineral Detection

Gas chromatography-mass spectrometry (GC-MS) technology was used to analyze the fatty acids in catfish muscle tissue both qualitatively and quantitatively. Using area normalization technique and the GB 5009.168-2016 [18] standard as a guide, a quantitative study of the relative fatty acid content was carried out. The GB 5009.268-2016 [19] standard is used to determine the mineral components in catfish muscle. To fully break down organic matter and transform minerals into soluble ions, muscle samples are treated with either wet digestion or dry ashing. Atomic absorption spectroscopy (AAS), inductively coupled plasma optical emission spectroscopy (ICP-OES), or flame photometry are used to determine each mineral's composition, which is then measured using the standard curve approach [20].

2.4. Metabolomics Analysis

Channel catfish muscle samples were snap-frozen in liquid nitrogen after dissection. Approximately 80 mg of tissue was transferred to a 2 mL Eppendorf tube on dry ice, followed by the addition of 200 µL H_2O and five ceramic beads for homogenization. Metabolites were extracted with 800 µL of methanol/acetonitrile (1:1, *v*/*v*), and the mixture was centrifuged (14,000× *g*, 4 °C, 15 min). The supernatant was dried under vacuum and reconstituted in 100 µL of acetonitrile/water (1:1, *v*/*v*) for LC-MS analysis.

Analysis was conducted using a UHPLC system (Agilent 1290 Infinity LC, Agilent Technologies, Inc., Santa Clara, CA, USA) coupled to a quadrupole time-of-flight mass spectrometer (Sciex TripleTOF 6600, SCIEX, Framingham, MA, USA). Separation was achieved on an ACQUITY UPLC BEH column (2.1 mm × 100 mm, 1.7 μm) with a mobile phase consisting of (A) 25 mM ammonium acetate and 25 mM ammonium hydroxide in water and (B) acetonitrile. The gradient program was as follows: 85% B (1 min), decreased linearly to 65% B (11 min), then to 40% B (0.1 min) and held for 4 min, returned to 85% B (0.1 min), followed by 5 min re-equilibration. Data were acquired in both ESI positive and negative modes.

Raw MS data were converted to mzXML format using ProteoWizard MSConvert and processed in XCMS. Peaks were detected with the centWave algorithm [*m*/*z* tolerance = 10 ppm, peakwidth = (10, 60)], then grouped [bw = 5, mzwid = 0.025, minfrac = 0.5]. CAMERA was used for isotope and adduct annotation. Features detected in over 50% of samples in at least one group were retained. Metabolite identification was based on accurate mass (*m*/*z* error < 10 ppm) and MS/MS matching against an in-house database of authentic standards. Missing values were imputed via the KNN method, and extreme values were removed. Data were normalized by total peak area to ensure comparability.

2.5. Proteomic Analysis

Peptide mixtures were redissolved in 20 mM ammonium formate (pH 10.0) and fractionated using high-pH reverse-phase separation on an XBridge C18 column (4.6 mm × 250 mm, 5 μm) connected to an Ultimate 3000 system. Separation was performed over a 40-min linear gradient at a flow rate of 1 mL/min and 30 °C. The collected fractions were desalted, vacuum-dried, and then redissolved in 0.1% formic acid for LC-MS/MS analysis.

LC-MS/MS was conducted using an EASY-nLC 1200 system coupled online to an Orbitrap Fusion Lumos mass spectrometer (Thermo Fisher Scientific, Waltham, MA, USA). Peptides were loaded onto an Acclaim PepMap C18 column (75 μm × 25 cm) and separated with a 120-min gradient of 5–35% acetonitrile in 0.1% formic acid at a flow rate of 200 nL/min, with an electrospray voltage of 2.0 kV.

The mass spectrometer operated in data-dependent acquisition mode. Full MS scans (*m*/*z* 350–1500) were acquired at a resolution of 120,000, with an AGC target of 4×10^5 and a maximum injection time of 50 ms. MS/MS scans were performed via HCD fragmentation at a resolution of 15,000, with an AGC target of 5×10^4, maximum injection time of 35 ms, and collision energy of 32%.

For data analysis, the raw files were processed using Spectronaut 18.4 (Biognosys AG) against the Uniprot database. Trypsin was specified as the enzyme, and the false discovery rate (FDR) was set to 1% at both the peptide and protein levels. Protein quantification was based on the average peak area of the top three peptide precursors.

2.6. Integrative Analysis of Metabolomics and Proteomics

Differential metabolites (DMs) (*p*-values ≤ 0.05 and VIP ≥ 1) and differentially expressed proteins (DEPs) (FDR < 0.05 and |log2 FC| > 1) were used for integrative analysis of control and salinity groups. The Pearson method was used to analyze the correlation coefficient of data between metabolomics and proteomics by the R package. A heatmap was used to show the connection between DMs and DEPs. All computational analyses were performed on a standard workstation equipped with an Intel Xeon Gold 6248R processor, 64 GB RAM, and one GPU for Spectronaut acceleration. The metabolomics raw data processing (ProteoWizard + XCMS + CAMERA) for 18 samples required approximately 2 CPU-hours; proteomics database searching and quantification (Spectronaut X) required approximately 4 CPU-hours; O2PLS integration analysis (OmicsPLS R package) required approximately 0.5 CPU-hours; trend analysis (STEM) required approximately 0.2 CPU-hours; and all statistical analyses and visualizations in R required less than 0.1 CPU-hours. The total computational time for the entire analysis pipeline was approximately 7–8 CPU-hours.

2.7. Statistical Analysis

Statistical analyses for all data were carried out in R 3.3.1 software (https://www.r-project.org/, accessed on 23 April 2025). The results are expressed as means ± standard error. Two-tailed unpaired *t*-test and one-way analysis of variance (ANOVA) with Tukey's multiple comparison test were utilized to analyze the significance of differences between groups. Results were presented as the means ± standard deviation (S.D.), asterisks (*) indicate statistically significant differences between the salinity group and control group, * $p < 0.05$ and ** $p < 0.01$, "NS" indicates no statistically significant differences between the salinity group and control group, $p > 0.05$.

2.8. Trend Genes Analysis

To better understand the stress and change mechanisms of fish fry under salt stress, we performed trend analysis on differentially expressed genes matching the differentially expressed proteins to further examine changes in DEP expression across the three groups. A technique for grouping gene expression patterns according to the features of several continuous samples is trend analysis. From the clustering findings, choose gene sets that exhibit certain biological traits. Use the ShortTime-series Expression Miner [21] to analyze trends.

3. Results

3.1. Effects of Salinity Stress on Biochemical Parameters

Each stage of the experiment lasted eight weeks and was separated into two phases: the stress stage and the de-stress stage (Figure 1A). The body weight data of the CG, LG, and HG groups were monitored throughout the experiment. The weight increase rate at each stage was then calculated and displayed as a line chart (Figure 1B,C). According to the results, the control group's (CG) body weight was significantly higher than the high salt group's (HG, $p < 0.05$) during the salt stress period. However, there was no significant difference with the low salt group (LG), and the weight gain rate was in line with the weight trend. From the 10th to the 12th week and the 14th to the 16th week, respectively, the low salt group and the high salt group had greater weight gain efficiency during the de-stress stage than the previous phases. Following the 12th week, the low-salt group's weight gain rate grew continuously and was greater than the control group.

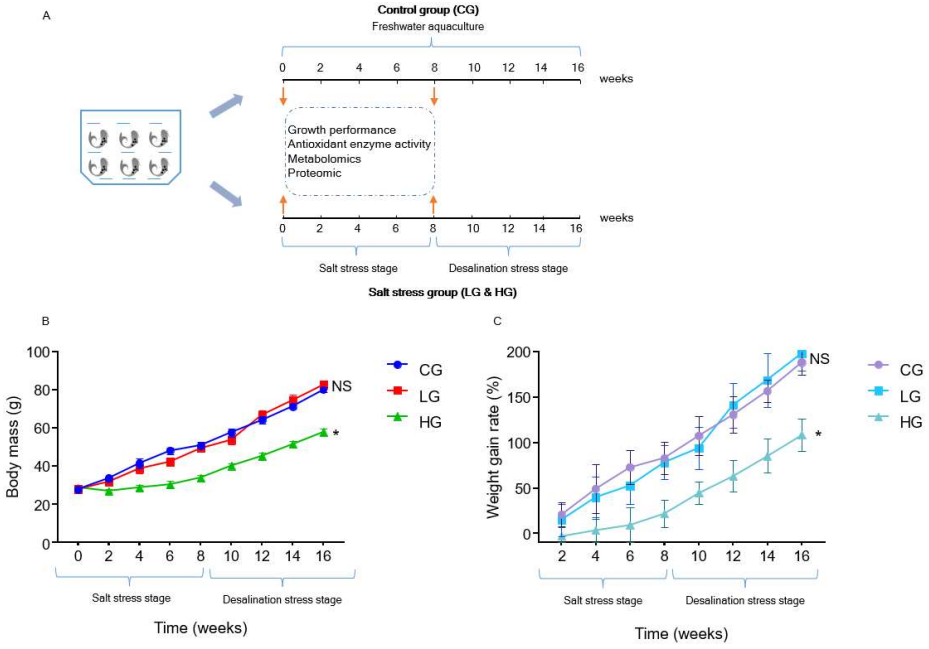

Figure 1. The growth differential between the high salt group (HG), low salt group (LG), and control groups (CG). (**A**) Main technical plan; (**B**) Differences in weight increase between the salinity groups and control groups; (**C**) Differences in weight gain

rate between salinity groups and control groups. * indicate significant differences ($p < 0.05$), NS indicate no significant differences ($p > 0.05$).

The muscle tissues of different catfish groups were used in this experiment to identify fatty acids and mineral elements, and a total of 77 associated indications were found. Of them, 27 effective detection indicators were found, with a detection rate of 35.1%; 4 indicators had substantial differences, making up 14.8% of the effective detection indicators; and 50 indications were not found, making up 64.9% of all detected indicators. Four indicators—Na, Mg, K, and Se—showed notable variations in the mineral element identification findings. While the Na content in the HG group was 32.48% greater than that in the CG group (Figure 2A, $p < 0.01$), the Na content in the LG group was comparable to that in the CG group. There is no discernible difference between salinity groups, and the trend of Mg and K content changes in each salinity treatment group is consistent with significant increases (Figure 2B,C, $p < 0.05$), the Se content significantly increased with increasing salinity (Figure 2D, $p < 0.05$), demonstrating a clear dose-response relationship. The results of fatty acid testing showed that none of the indicators reached statistical significance, but some components showed a certain trend of change (Figure 2E, $p > 0.05$). In terms of polyunsaturated fatty acids (PUFAs), the three groups' contents of C18:2n6c (linoleic acid) ranged from 25.33% to 25.63%; C18:3n3 (α-linolenic acid) was slightly higher in the HG group (2.53%) and slightly lower in the LG group (2.08%); and C22:6n3 (DHA) was highest in the CG group (2.58%) and lowest in the HG group (2.17%). While major saturated fatty acids like C16:0 and C18:0 did not exhibit significant salt-dependent changes, the content of saturated fatty acids (SFA, calculated as fat) remained relatively stable in all three groups; the content of monounsaturated fatty acids (MUFA) was slightly higher in the HG group than in the other two groups, exhibiting a slight upward trend.

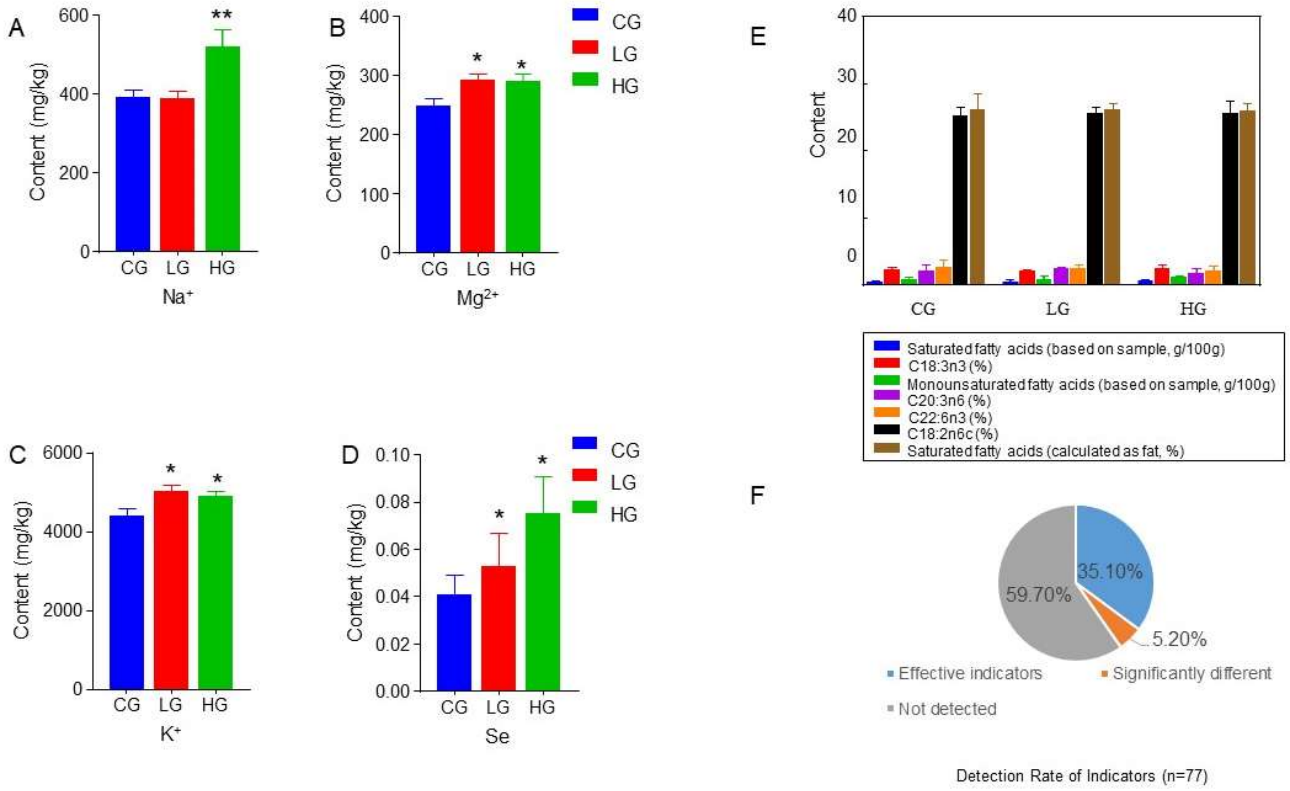

Figure 2. Variations in the content of mineral elements and fatty acids in the muscles of channel catfish subjected to salinity. (**A**) Na^+, (**B**) Mg^{2+}, (**C**) K^+, (**D**) Se, (**E**) Fatty acids content, (**F**) Detection rate of effective indicators. * indicate significant differences ($p < 0.05$), ** indicate significantly different ($p < 0.01$).

3.2. Metabolomics Analysis After Salt Exposure

3.2.1. Multivariable Statistics

The differences of metabolites in the channel catfish muscle were distinguished by multivariate statistical analysis, including PCA and OPLS-DA analysis. The PCA scores plot of the UPLC-QTOF-MS data in the positive and negative ion modes is shown in Figure 3A–D. The results showed that the metabolites between the salt and control groups were not well distinguished in the unsupervised principal component analysis model, which may be due to the limitations of the PCA model [22]. In contrast to the PCA model, OPLS-DA is a supervised model that extracts variable information and minimizes system noise. Consequently, compared to the PCA model, the OPLS-DA model has a more crucial classification capacity [23]. In the OPLS-DA scores plot, clear separation of the control and salt stress groups was obtained, suggesting that salinity treatment conspicuously perturbed muscle metabolite profiles (Figure 3E–H). The $R^2Y$and Q^2Y values of the low salt treatment group (LG) and high salt treatment group (HG) in positive ion mode were 0.851 and 0.583, 0.915 and 0.440, respectively, whereas those of the negative ion model were 0.846 and 0.506, 0.956 and 0.718, respectively, indicating that the OPLS-DA model fits well and is highly predictable and suitable for subsequent data analysis. Multiple permutation tests were used to permutation test (over-fitting verification) on the OPLS-DA model (Figure 3I–L). The results showed that the R^2 and Q^2 generated from the random permutations were higher than those of the original OPLS-DA model, indicating that the OPLS-DA model was reliable and valid and the developed models were not overfitted.

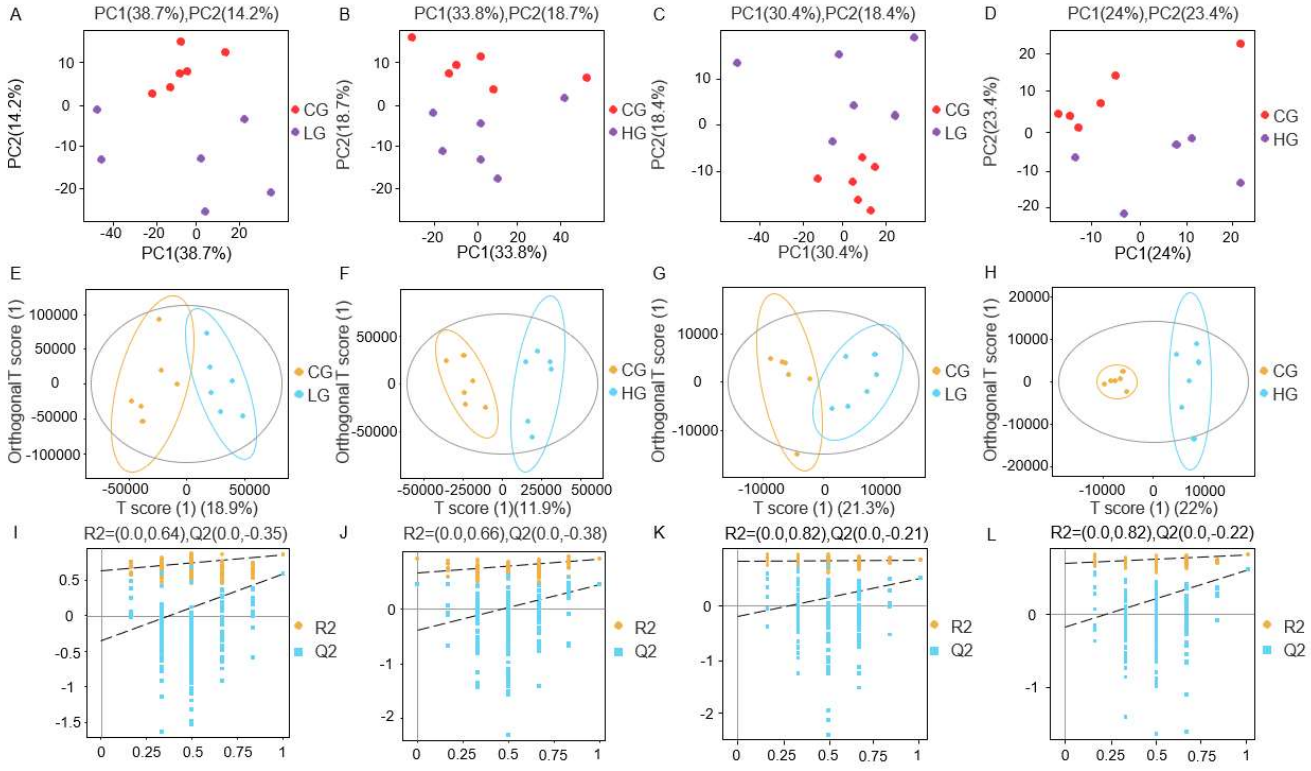

Figure 3. Quality analysis of metabolomics data. (**A**,**B**) The PCA scores plot of samples acquired in the positive ion mode. (**C**,**D**) The PCA scores plot of samples acquired in the negative ion mode. (**E**,**F**) The OPLS-DA score plot for the positive ion mode. (**G**,**H**) The OPLS-DA score plot for the negative ion mode. (**I**,**J**) The OPLS-DA permutation test for the positive ion mode. (**K**,**L**) The OPLS-DA permutation test for the negative ion mode. Orange and blue points represent the R2 and Q2 values of each permutation, respectively. Orange and blue dashed lines indicate the linear regression trend lines for R2 and Q2. The black dashed line represents the intercept reference line of the regression models, which is used to assess the risk of overfitting (a lower intercept indicates a more robust model). The horizontal solid black line represents the reference line at y = 0.

3.2.2. Differential Enrichment Analysis

Ultimately, VIP > 1.0 and p-value < 0.05 were used to identify DMs between the salinity stress and control groups. In the positive ion mode, 25 DMs were found in the low salt group; 13 of them were up-regulated, and 12 were down-regulated when compared to the control group. Of the 74 DMs found in the high salt group, 40 were up-regulated, and 34 were down-regulated as compared to the control group (Figure 4A). Furthermore, 39 DMs were found in the low salt group in the negative ion mode; 26 of them were up-regulated, and 13 were down-regulated when compared to the control group. Of the 64 DMs found in the high salt group, 27 were up-regulated, and 37 were down-regulated when compared to the control group (Figure 4B).

A hierarchical cluster analysis was carried out to depict the content and relative relationships of the DMs (Figure 4C,D). The findings demonstrated that DMs in the salt and control groups differed significantly in color, suggesting that salt exposure had a major impact on channel catfish muscle metabolism in comparison to the control group. Among these, lipid metabolism was most dramatically altered. To identify the probable metabolic pathways influenced by salt exposure, we evaluated the DMs data from the control and salinity treatment groups. The findings demonstrated that a variety of metabolic pathways are impacted by salt stress, nevertheless, we determined that the metabolism of glycerophospholipid metabolism, arachidonic acid metabolism, linoleic acid metabolism, and alpha-Linolenic acid metabolism were the most pertinent metabolic pathways.

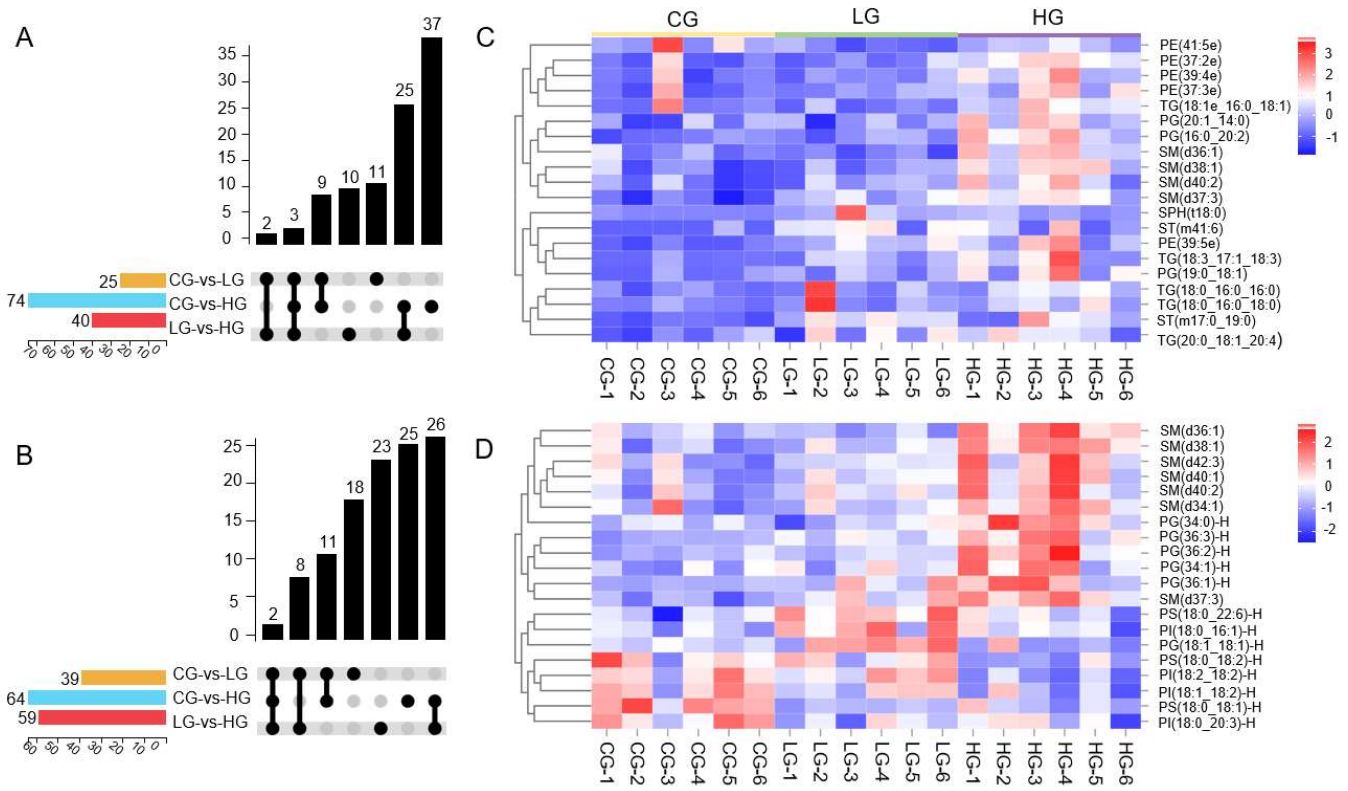

Figure 4. Differential metabolites analysis of metabolomics. Upset diagram (**A**) and differential metabolite clustering heat map (**C**) in POS ion mode; Upset diagram (**B**) and differential metabolite clustering heat map (**D**) in NEG ion mode.

3.3. Proteomic Analysis After Salt Exposure

3.3.1. Differential Protein Analysis

31,003 peptides containing 6026 proteins in the proteome. The peptide number distribution is presented in Figure S1. Violin plots are used in this work to visualize the expression of protein abundance among

samples (Figure 5A). In the meanwhile, a Venn diagram based on the quantity of proteins that were expressed differently between groups was used for visual examination (Figure 5B). Following salinity stress, 105 DEPs were detected in the muscle of the low-salinity group and 364 in the muscle of the high-salinity group. The muscle's low salt group had 47 substantially elevated proteins and 58 significantly downregulated proteins compared to the control group. Comparing the high salt group to the control group, 121 proteins were up-regulated, and 243 were down-regulated (Figure 5C). We displayed the differential proteins between the two groups using a volcano plot in order to better observe the expressing variations in the proteins between the control group and the salinity group (Figure 5D,E).

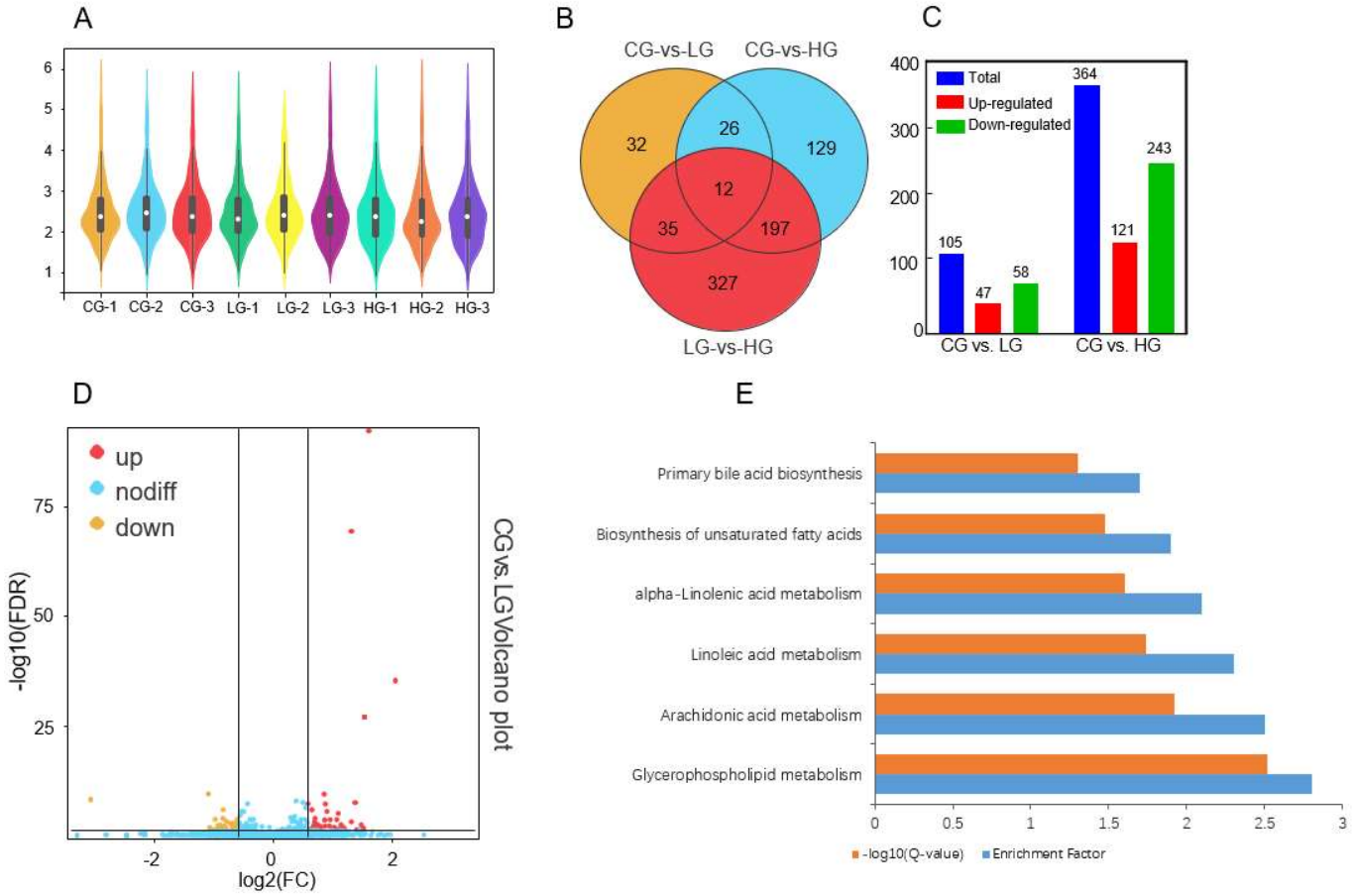

Figure 5. Differential protein analysis of proteomics. (**A**) Violin diagram, visualization of protein abundance expression; (**B**) Wayne diagram, showing the common and unique target proteins in different comparison groups; (**C**) The quantity of proteins that are differently expressed between groups and either up- or down-regulated; (**D**,**E**) Volcano map, showing the difference of proteins between the two groups.

3.3.2. GO Enrichment Analysis

We compared and annotated DEPs using the GO and KEGG databases, respectively. The GO database covers three biological terms, biological processes, molecular functions, and cellular components [24]. All DEPs were annotated in the GO database. The main DEP enrichment pathways were arranged according to *Q* values, where the *Q* value was the *p* value corrected by multiple hypothesis tests. Enrich and classify differentially expressed proteins, and use hypergeometric testing to identify significantly enriched GO terms in different comparison groups. Visualize the results using a secondary classification bar chart (Figure 6). In biological processes, the top five categories were cellular process, metabolic process, biological regulation, regulation of biological process, and response to stimulus. The main molecular function

categories were binding and catalytic activity. In cellular components, categories were represented by cellular anatomical entity and protein-containing complex.

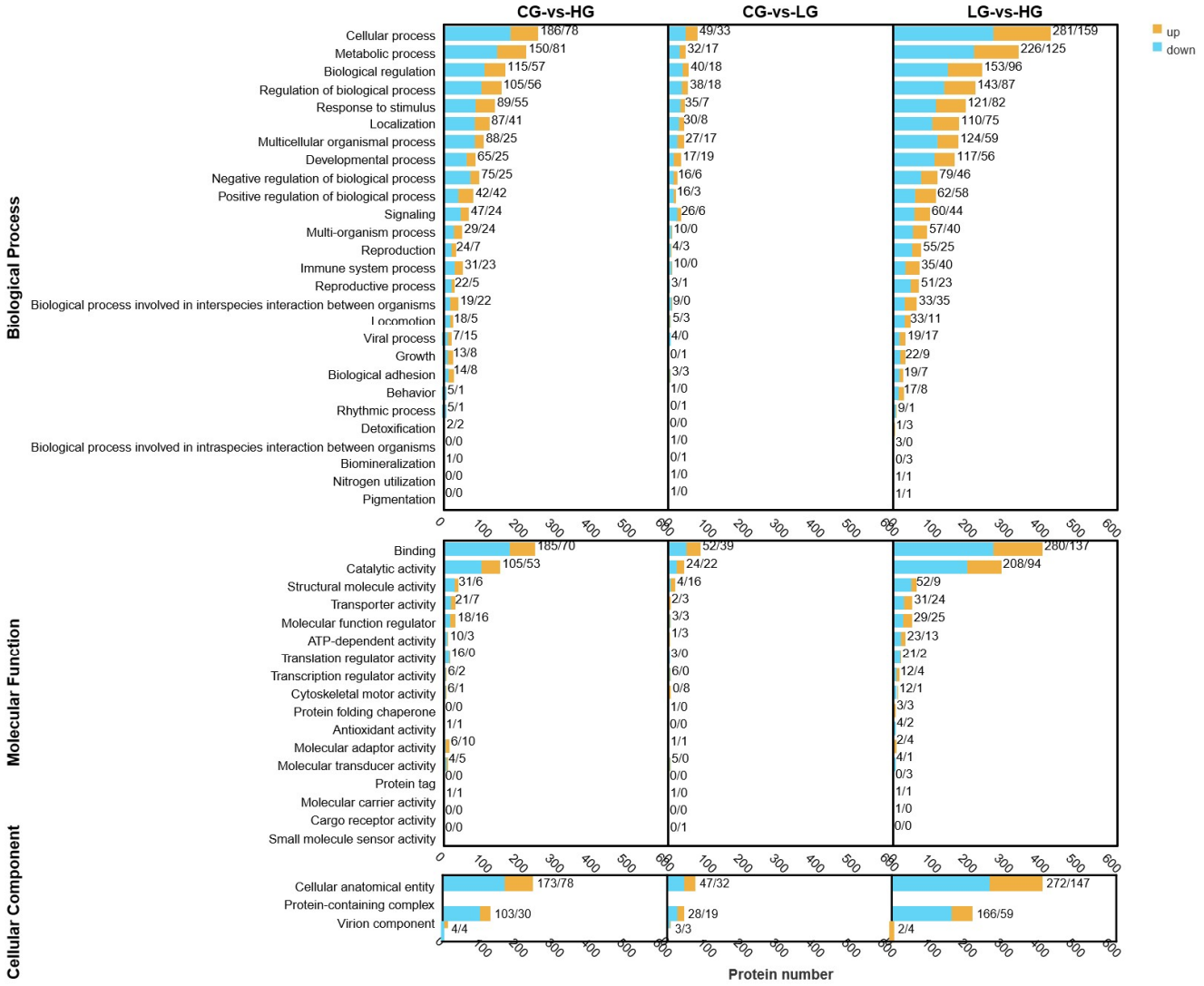

Figure 6. Go enrichment analysis diagram of differentially expressed proteins. The enrichment route is shown by the ordinate, while the number of differential proteins is represented by the abscissa. Blue denotes fall and yellow denotes growth in the figure.

After exposure to salinity stress, compared with the control group, the first three significantly enriched pathways in the low salt group were regulation of division septum assembly, regulation of cell septum assembly and regulation of cytokinetic process, which were consistent between low salt group and control group (Figure S2A). In addition, the most significantly enriched pathway in the high salt group was extracellular space (Figure S2B). Intriguingly, when we compared the enrichment pathways of the experimental and control groups, we found that all of the pathways that were significantly enriched in proteins that were differentially expressed between the high salt and low salt groups were associated with cell growth and differentiation. But when we compared the enrichment pathways of proteins that were differentially expressed between the low and high salt groups, we discovered that the majority of the pathways had to do with the body's metabolism of ribose and amino acids. The first three significantly enriched pathways were carboxylic acid metabolic process, nucleotide metabolic process, and organic acid metabolic process (Figure S2C). Table S1 displays all of the pathway codes seen in Figure S2.

3.3.3. KEGG Enrichment Analysis

The KEGG database provides insights on advanced functions and biological systems (cells, organisms, and ecosystems), genome sequencing, and other high-throughput experimental technologies from molecular information, especially large molecular datasets [25]. Map the differential protein set to the KEGG database, enrich and classify the differential proteins, and use hypergeometric testing to summarize significantly enriched DEP pathways ($Q < 0.05$). 133, 642, and 1040 differentially expressed proteins (DEPs) were found to be enriched in the L *vs*. C, H *vs*. C, and L *vs*. H groups, respectively. of which DEPs were classified according to the KEGG A_ hierarchy and enriched in pathways metabolism, human diseases, organismal systems, genetic information processing, cellular processes, and environmental information processing, respectively. The metabolism-related pathways that were enriched with proteins that were differently expressed were the most important of these. These primary pathways include carbohydrate metabolism, amino acid metabolism, lipid metabolism, energy metabolism, and so on (Figure 7).

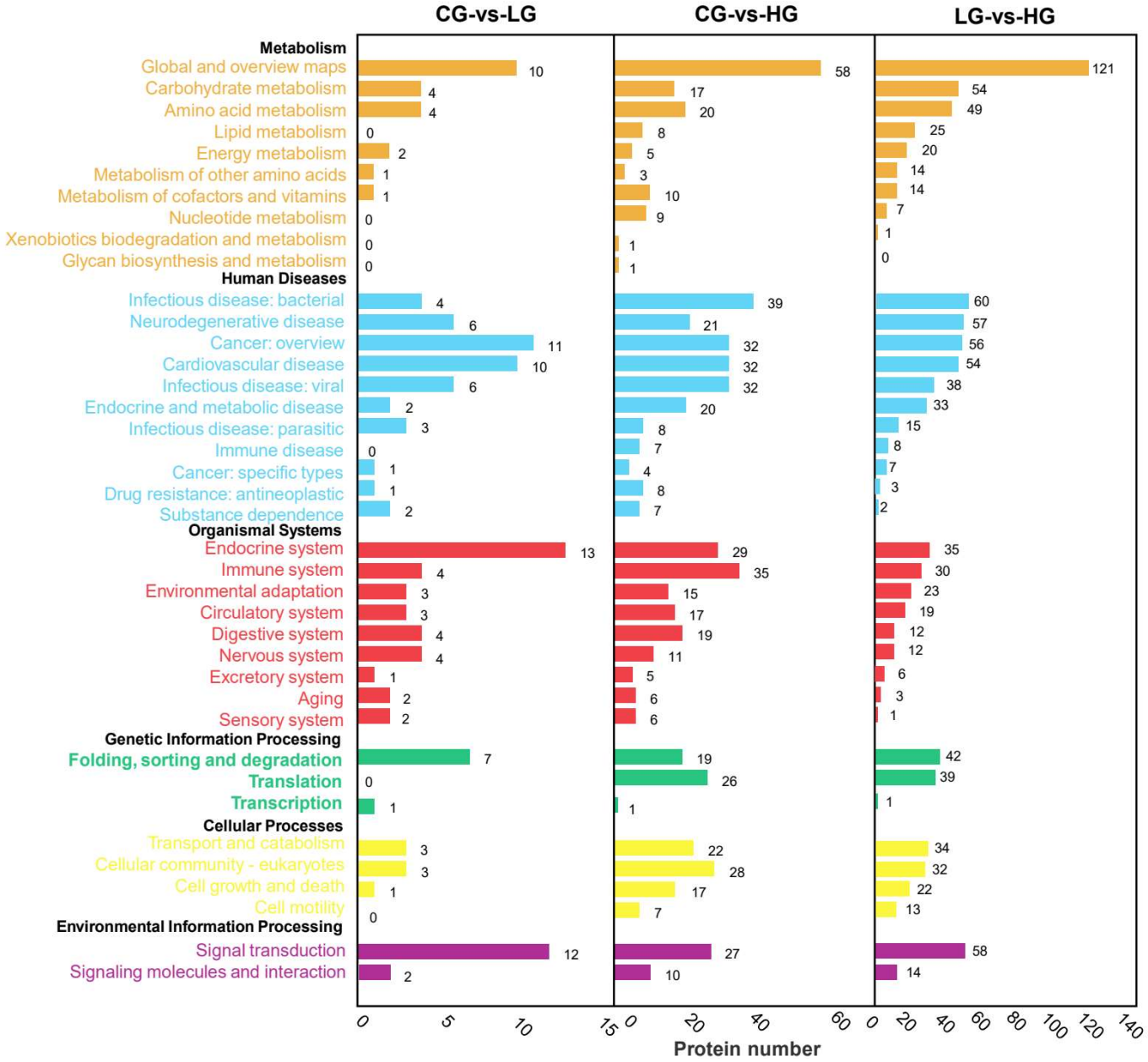

Figure 7. KEGG enrichment analysis diagram of differentially expressed proteins. The enrichment route is shown by the ordinate, while the number of differential proteins is represented by the abscissa.

From FDR values, the top 20 KEGG pathways enriched by DEPs from LG *vs*. CG, HG *vs*. CG, and LG *vs*. HG comparisons were generated. Of these, pathways enriched in the LG were mainly enriched for metabolism-related pathways (glycine, serine and threonine metabolism, cholesterol metabolism, and nitrogen metabolism), and immune disease-related pathways (thyroid hormone signaling pathway, protein processing in endoplasmic reticulum, central carbon metabolism in cancer, dilated cardiomyopathy, hypertrophic cardiomyopathy, and so on) (Figure S3A). Meanwhile, the pathways enriched in HG mainly include immune disease-related pathways (e.g., cortisol synthesis and secretion, vascular smooth muscle contraction and viral myocarditis) as well as the biosynthesis of fatty acids and amino acids (Figure S3B). As before, we also contrasted the enrichment pathways of proteins that were differently expressed in the HG and LG experimental groups. We were shocked to discover that, in contrast to the enrichment pathway in Figure S3A,B, the DEPs enriched pathway in Figure S3C was linked to several metabolic pathways, including the aminoacyl tRNA biosynthesis, valine, leucine, and isoleucine degradation, fatty acid metabolism, and fatty acid elongation relevant. Table S2 displays all of the pathway codes seen in Figure S3.

3.3.4. Trend Genes Analysis

We computed *p*-values using hypothesis testing and performed KEGG/GO functional enrichment analysis on genes in different trends. KEGG/GO that satisfies the criterion of *Q*-value < 0.05, as determined by the *p*-value obtained after FDR correction [26], are considered highly enriched in this trend. Following the trend-based normalization of the 758 gene data, trend patterns were created. 8 trend pattern graphs were created (Figure 8A). Furthermore, we created a histogram using the number of genes as the ordinate and the color of the column as the *p* value. We thoroughly examine the mechanism of salt stress in conjunction with the trend pattern (Figure 8B). The eight trend pattern maps also differ in the primary roles played by each trend gene enrichment pathway. The trend gene enrichment pathway in profile 0 is primarily responsible for preserving the body's osmotic equilibrium. Enrichment pathways in profiles 1 and 2 are mostly associated with energy generation, consumption, storage, metabolism, and growth balance. Numerous metabolic activities (including fatty acid synthesis, breakdown and extension, amino acid intake and energy supply, gluconeogenesis and glycolysis, *etc*.) are intimately linked to the enrichment pathways seen in profiles 3 and 5. The immune response and signal transduction are associated with the enrichment pathways of trend genes in profiles 4, 6, and 7. When paired with Figure 8B, it is evident that the primary ways that salinity affects catfish are through fatty acid metabolism, osmotic pressure homeostasis, and some immunological functions. In general, this outcome is in line with the one from the earlier phase.

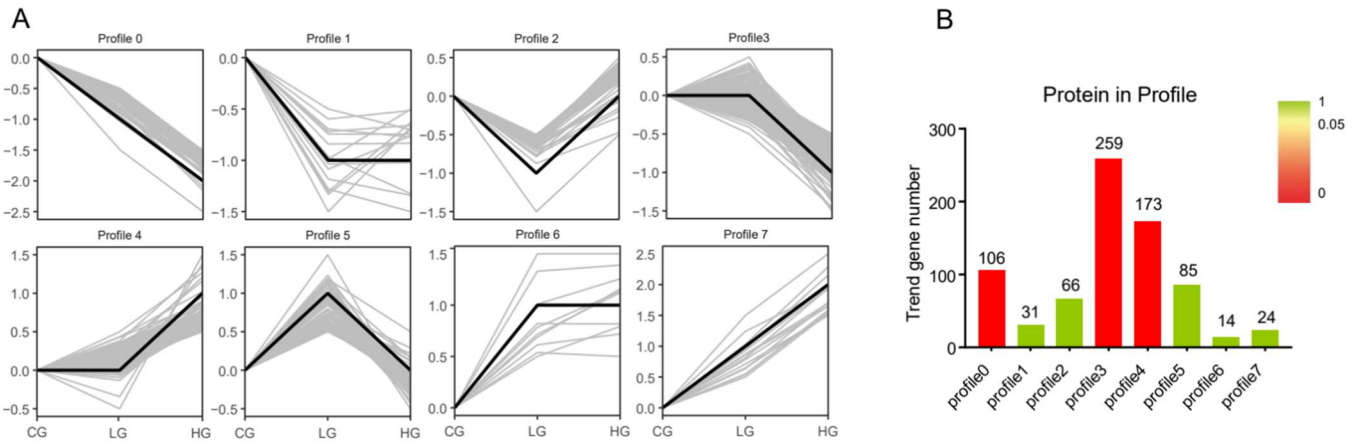

Figure 8. Trend gene analysis. (**A**) Trend pattern chart: create each trend pattern chart after normalizing the gene data based on the trend. The trend line is shown by the black line, and each gene is shown by the gray line. (**B**) *p*-value histogram: the color of the column indicates the *p*-value, and the height of the column indicates the number of genes.

3.4. Integration Analysis of Multi-Omics Data

Integrated analysis was applied to further investigate the catfish muscle response to salinity stress. A heat map showing the link between DEP and DEM among the top 250 correlation coefficients of catfish muscle was created based on the thorough examination of differentially expressed proteins and metabolites (Figure 9A). In parallel, a network map was created for the metabolites and differential proteins that ranked in the top 250 and had absolute correlation values higher than 0.5 (Figure 9B). Between the CG and HG groups, there were 64 differentially enriched proteins and 2 differentially enriched metabolites. Of these, 58 differentially enriched proteins and 1 metabolite were enriched via the glycolysis/gluconeogenesis pathway, while the remaining proteins and metabolites were enriched via retrograde endocannabinoid signaling. Remarkably, after thorough investigation, we could not identify any pertinent enrichment pathways between the CG and LG groups. Alpha-Linolenic acid metabolism, retrograde endocannabinoid signaling, choline metabolism in cancer, and metabolic pathways were among the 131 DEPs and 6 DEMs that we also compared between the two salinity groups. A total of 121 DEPs and 1 DEM are enriched in the metabolic route out of the four pathways; the remaining DEPs and DEMs are enriched in the other pathways.

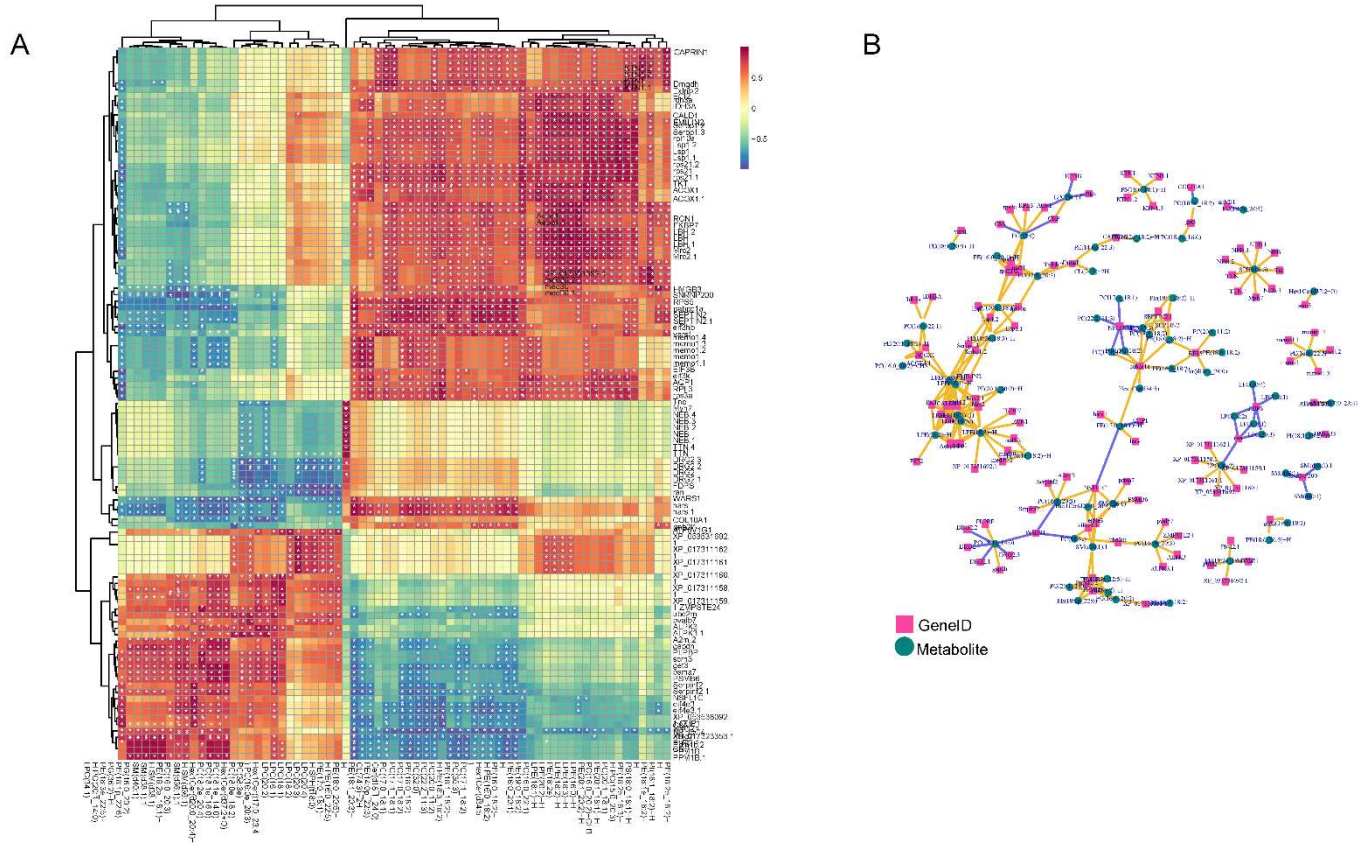

Figure 9. Integration analysis of multi-omics data. (**A**) Thermogram of correlation between protein expression and metabolite abundance, the ordinate denotes differential proteins, whereas the abscissa denotes differential metabolites. (**B**) Network diagram of correlations between protein expression and metabolite abundance; the pink box represents the Gene ID, and the green circle represents the Metabolite.

Based on all proteome and metabolomics data, we conducted O2PLS analysis using the OmicsPLS tool [27]. The O2PLS model is suitable for correlation analysis of two omics data and is capable of bidirectional modeling and prediction in two data matrices. We created loading plots for various omics variables in the joint section to clarify the relationship between proteins and metabolites under salinity stress. The findings show a negative correlation between the majority of DEMs and DEPs and another set of studies. It's also noteworthy that, in this omics, DEMs had a largely positive correlation, but DEPs

showed the exact opposite pattern (Figure 10A,B). The top 25 proteins and metabolites with the square sum of the loading values in the first two dimensions were chosen based on the loading value results, and they were then combined to create a loading graph. The majority of DEMs are enriched on the positive axis within omics, as shown in Figure 10A, whereas DEPs are enriched on the negative axis within omics (Figure 10C). Further confirm the reliability of the loading plot.

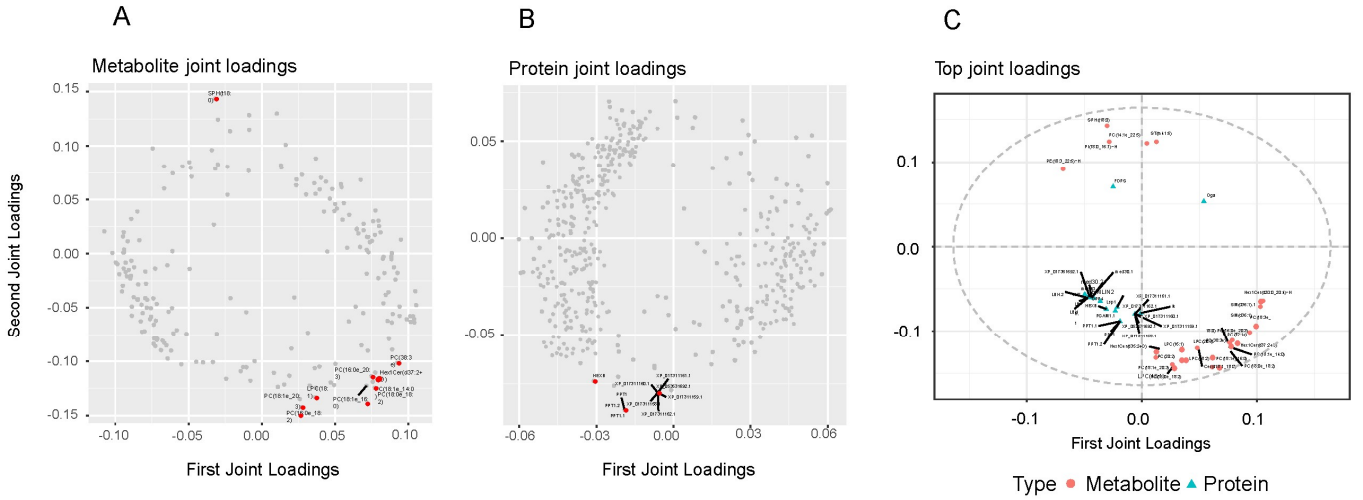

Figure 10. O2PLS model analysis diagram. (**A**) Metabolomics O2PLS load map; (**B**) Proteomics O2PLS load map; (**C**) Omics load diagram, positive correlation is represented by the positive axis on the coordinate axis, whereas negative correlation is represented by the negative axis.

4. Discussion

By combining standard biochemical methods with data-independent acquisition-based proteomics and LC-MS/MS-based untargeted metabolomics, this work offers new insights into the molecular pathways underlying the muscle response of channel catfish to prolonged exposure to salt. Under salt stress, the antioxidant system and lipid metabolism were disrupted, and multiple metabolic pathways were affected, further inducing cell apoptosis and disease immune response. Collectively, this study examined the molecular level of the stressful effects of salt on channel catfish muscle tissues. Our knowledge of catfish tolerance mechanisms under salinity stress is shaped in part by the information provided here. At the same time, it was underlined how crucial it is to apply the multi-omics method and biochemical tests in tandem to better comprehend salty environmental stress.

4.1. Omics Analysis

Salinity changes in aquatic habitats can result in aberrant lipid metabolism in aquatic animals [28]. Research indicates that salt stress impacts various lipid metabolic pathways, including cholesterol metabolism, fat digestion and absorption, fatty acid biosynthesis, cholesterol metabolism, insulin resistance, and PPAR signaling pathways [7,29,30]. In this study, metabolomics data showed that salt stress significantly changed the lipid homeostasis of catfish muscles. After 8 weeks of salt stress in 5 psu (LG) and 9 psu (HG), the metabolic pathways related to lipid metabolism, including glycerophospholipid metabolism, arachidonic acid metabolism, linoleic acid metabolism, and alpha-Linolenic acid metabolism, were significantly altered. In the field of proteomics, KEGG enrichment analysis revealed that the differentially expressed proteins (DEPs) in the salinity group compared to the control group were only partially associated with metabolic pathways, these included the PPAR signaling pathway, cholesterol metabolism, and fatty acid biosynthesis. Furthermore, various metabolic pathways, including carboxylic acid metabolic process, valine, leucine, and isoleucine degradation, fatty acid degradation, aminoacyl-

tRNA biosynthesis, etc., were linked to differently expressed proteins in the two salinity groups (LG group and HG group), according to KEGG and GO enrichment analyses. Furthermore, GO enrichment analysis of the proteomics data revealed significant alterations in pathways related to cell division, protein digestion, and absorption in both salinity-exposed groups compared to the control group. These findings further suggest that salinity exposure influences protein metabolism, as well as cell division and differentiation processes, to a certain extent. Notably, we observed a high degree of consistency in the enriched pathways of differentially expressed proteins (DEPs) between the low salinity (LG) and high salinity (HG) groups, which partially diverges from the earlier experimental results of this study. The majority of the differential metabolites between the salinity group and the control group were elevated, according to the combined proteome and metabolome study; however, the majority of the differential proteins were downregulated. Based on this phenomenon, we hypothesize that the aberrant accumulation of certain metabolites under salt stress will feedback inhibit the translation of related enzymes' genes or proteins in the synthesis pathway; in other words, the higher the metabolite concentration, the more strongly upstream proteins are inhibited, which results in a decrease in the expression of these proteins. Unfortunately, we were unable to pinpoint the specific differential proteins or metabolites that were responsible for this event; hence, more research is required to confirm this theory.

4.2. Fatty Acid and Mineral Element Analysis

An essential connection between fish physiology, aquaculture, food safety, and the ecological environment is the identification of mineral elements in fish muscles. Changes in the various mineral elements' contents in their muscles are crucial markers for fish aquaculture that is healthy [31]. Important ions that preserve cell osmotic pressure and membrane potential include sodium (Na^+) and potassium (K^+) [32,33]. Magnesium ions are coenzymes for more than 300 enzymes involved in a variety of processes, including energy metabolism and nucleic acid synthesis, and they also take role in the control of enzyme activity [34,35]. Glutathione peroxidase (GSH-PX) requires selenium [36,37]. To maintain normal physiological function and adjust to variations in ambient salinity, the salinity treatment group of fish fry in this experiment had higher Na and K contents. While the increase in Se content with rising salinity improved the antioxidant and defense capabilities of the fish fry themselves, which is a crucial protective mechanism for fish to deal with salinity stress, the increase in Mg content improved aerobic metabolism and met energy requirements. Analyzing the physiological metabolism, nutritional requirements, and ecological adaptation of fish, as well as ensuring aquaculture efficiency, assessing the nutritional safety of aquatic products, directing human health consumption, and safeguarding fishery resources, all depend on the detection of fatty acids in fish muscle [38,39]. Polyunsaturated fatty acids (PUFAs), such as DHA and EPA, preserve the fluidity and functionality of cell membranes [40,41]. In fish, monounsaturated fatty acids (MUFA) and saturated fatty acids (SFA) are significant sources of energy [42–44]. The experiment's salinity group's fatty acid content only revealed a modest tendency of change and did not exhibit statistically significant variations in fatty acid-related markers when compared to the control group. We hypothesize that this outcome may be due to the fact that fish fry become more resilient to salt stress as they become older, and their self-defense system lessens the effects of metabolic abnormalities brought on by salt stress.

The dynamic changes of mineral elements in fish muscle tissue can shed additional light on how fish adjust to high salt environments under salt stress from the perspective of ion homeostasis regulation. To maintain a stable internal environment and cope with high salt stress, fish may also modify the functional activity and subcellular localization of ion channel proteins and signaling pathway-related proteins, in addition to initiating adaptive responses like increased energy metabolism and activation of antioxidant defense systems. The aforementioned adaptive response characteristics are very consistent with the main pathways enriched by differential metabolites and proteins in the combined research of metabolomics and

proteomics. In the subsequent mechanism validation and comprehensive research, metabolomics should focus on the quantitative detection of metabolites at significant energy metabolism nodes, targeted analysis of metabolic pathways associated with the antioxidant system, and dynamic monitoring of important intermediate products in fatty acid metabolism. At the proteomic level, it is crucial to focus on the expression and post-translational modification characteristics of functional proteins associated with ion transmembrane transport, carefully analyze the expression patterns and activity changes of significant magnesium and selenium-dependent enzymes, and fully explore the regulatory functions and molecular mechanisms of antioxidant proteins and stress response proteins in fish salt stress adaptation.

4.3. Trend Genes Analysis and Reduction of Salt Stress

As previously stated, we have confirmed time and time again in earlier research that catfish under salt stress suffer from oxidative stress and metabolic problems [45,46]. Fish are affected by salinity stress in a variety of ways, such as immunological damage, metabolic problems, energy imbalance, cellular macromolecule repair and protection, and more [47,48]. Currently, the aforementioned factors account for the majority of the effects of salinity on fish. Similar to the last experiment, we found that the salinity group's and the control group's differential enrichment pathways centered on metabolism, energy consumption, oxidative damage, and partial immune response in the trend enrichment analysis of differential proteins. In contrast to the control group, the high salt group's metabolic activity decreased abnormally, the genes related to the immune pathway increased significantly, and the energy supply of branched chain amino acid decomposition decreased. The difference is that the low salt group and the control group differ less at this stage of the test, with only a significant change in the enrichment zone of maintaining osmotic balance. This phenomena is in line with how each group's body weight and pace of weight growth changed during the stress phase. At this point, the high salt group is growing slowly. We hypothesize that it is brought on by an imbalance in energy use and the requirement to use more energy in order to keep the body's osmotic homeostasis. After the stress was removed, the salinity group showed a faster rate of development over time, indicating that the impact of salinity on catfish growth was progressively diminished and reversible as fry grew.

5. Conclusions

The key findings of this study are summarized as follows:

(1) Salinity stress perturbs lipid metabolism, oxidative balance, osmotic homeostasis, and immune response in channel catfish skeletal muscle. Integrated proteomic and metabolomic analyses identify glycerophospholipid metabolism, fatty acid synthesis/degradation/elongation, and branched-chain amino acid degradation as core affected pathways, consistent with the biochemical detection of elevated Na^+, K^+, Mg^{2+}, and Se levels and altered fatty acid profiles.

(2) High salinity (9 psu) induces broader and more severe effects than low salinity (5 psu). Trend analysis reveals that osmotic homeostasis is disrupted by both salinity levels, whereas metabolic disorders, energy utilization imbalance, and immune response gene up-regulation are specific to the high-salinity group. The low-salinity group shows no significant differences from the control in most pathways beyond osmotic regulation.

(3) The de-stress experiment demonstrates that salinity-induced growth suppression and metabolic disruption are largely reversible. Following the return to freshwater, both salinity groups exhibit accelerated weight gain, indicating compensatory growth and confirming that the damage incurred during the stress phase is reparable rather than permanent.

(4) These findings provide practical guidance for channel catfish aquaculture in saline-alkaline waters. Low-salinity conditions (5 psu) appear tolerable for juvenile channel catfish with minimal long-term impact, supporting the feasibility of expanding cultivation to brackish and low-salinity inland regions.

Supplementary Materials

The following supporting information can be found at: https://www.sciepublish.com/article/pii/1332, Figure S1: caption Peptide Number Distribution; Figure S2: GO enrichment pathways; Figure S3: KEGG enrichment pathways; Table S1: GO enrichment pathways; Table S2: KEGG enrichment pathways.

Statement of the Use of Generative AI and AI-Assisted Technologies in the Writing Process

During the preparation of this manuscript, the author used Deepseek in order to English polishing. After using this tool, the author reviewed and edited the content as needed and takes full responsibility for the content of the published article.

Author Contributions

Y.D.: Investigation, Experimentation, Data interpretation, Validation, Writing—original draft, Writing—review & editing; L.T.: Experimentation, Data validation, Writing—review & editing; H.L.: Experimentation, data validation, reviewing and editing; J.L.: Experimentation, Reviewing; M.W.: Project administration, Writing—reviewing & editing; L.Z.: Data interpretation, Reviewing and editing; X.C.: Resources, Funding acquisition, reviewing & editing; S.Z.: Conceptualization, Funding acquisition, Supervision, Writing—reviewing & editing.

Ethics Statement

All experiments were performed in accordance with the Regulations of the Animal Ethics Committee and were approved by the Institutional Review Board on Bioethics and Biosafety of Freshwater Fisheries Research Institute of Jiangsu Province (No. FT, 22003, 26 May 2024).

Informed Consent Statement

Not applicable.

Data Availability Statement

The metabolome data and proteomic data that support the findings are already deposited and will be available on the OMXI (https://ngdc.cncb.ac.cn/omix/preview/hZpU0JMNKe, OMIX ID is OMIX023303, accessed on 1 October 2026) and PRIDE (Project accession: PXD087280, Token: Y13AUQI4YZg8) under the accession number and following an embargo from the date of publication. They can be transferred to the reviewers upon editor request.

Funding

The study was funded by the National Key Research and Development Program of China (2024YFD2400905) and the earmarked fund for CARS (CARS-45).

Declaration of Competing Interest

The authors declare that they have no known competing financial interests or personal relationships that could have appeared to influence the work reported in this paper.

References

1. Zeng L, Ai CX, Wang YH, Zhang JS, Wu CW. Abrupt salinity stress induces oxidative stress via the Nrf2-Keap1 signaling pathway in large yellow croaker Pseudosciaena crocea. *Fish. Physiol. Biochem.* **2017**, *43*, 955–964. DOI:10.1007/s10695-016-0334-z
2. Zhang Y, Yu H, Chen H, Wang X, Tan Y, Sun J, et al. Integrative transcriptomic and metabolomic analyses reveal preliminary molecular mechanisms of gills response to salinity stress in *Micropterus salmoides*. *Aquaculture* **2025**, *606*, 742600. DOI:10.1016/j.aquaculture.2025.742600
3. Eissa N, Wang H. Transcriptional stress responses to environmental and husbandry stressors in aquaculture species. *Rev. Aquac.* **2016**, *8*, 61–88. DOI:10.1111/raq.12081
4. Xiong Y, Dong S, Huang M, Li Y, Wang X, Wang F, et al. Growth, osmoregulatory response, adenine nucleotide contents, and liver transcriptome analysis of steelhead trout (*Oncorhynchus mykiss*) under different salinity acclimation methods. *Aquaculture* **2020**, *520*, 734937. DOI:10.1016/j.aquaculture.2020.734937
5. Zhou Z, Hu F, Li W, Yang X, Hallerman E, Huang Z. Effects of salinity on growth, hematological parameters, gill microstructure and transcriptome of fat greenling *Hexagrammos otakii*. *Aquaculture* **2021**, *531*, 735945. DOI:10.1016/j.aquaculture.2020.735945
6. Yan J, Chen M, Wu K, Li Y, Hu J, Zhao W, et al. Effect of salinity and pH on oxygen consumption rate and ammonia excretion rate in asian moonscallop *Amusium pleuronecte*. *Fish. Sci.* **2018**, *37*, 181–186. DOI: 10.16378/j.cnki.1003-1111.2018.02.006
7. Liu Z, Ma A, Yuan C, Zhao T, Chang H, Zhang J. Transcriptome analysis of liver lipid metabolism disorders of the turbot *Scophthalmus maximus* in response to low salinity stress. *Aquaculture* **2021**, *534*, 736273. DOI:10.1016/j.aquaculture.2020.736273
8. Zhang J, Ding Q, Lou R, Zhang Y, Yao Y, Yang Y, et al. Stress Nutrition in Aquatic Animals: From Definition to Practice. *Rev. Aquac.* **2026**, *18*, e70091. DOI:10.1111/raq.70091
9. Zhong L, Song C, Chen X, Deng W, Xiao Y, Wang M, et al. Channel catfish in China: Historical aspects, current status, and problems. *Aquaculture* **2016**, *465*, 367–373. DOI:10.1016/j.aquaculture.2016.09.032/
10. China Agriculture Press. *China Fishery Statistical Yearbook*; China Agriculture Press: Beijing, China, 2024; pp. 42. Available online: https://cdn.theoutlawocean.com/inv/food-for-feed/doc/2024-china-fisheries-statistical-yearbook-2024-pdf.pdf
11. Zhong LQ, Wang MH, Chen XH, Zhang SY, Jiang HC, Bian WJ, et al. Current status and development strategy of the channel catfish industry in Jiangsu. *Chin. Agric. Sci. Bull.* **2021**, *37*, 137–143. Available online: https://iac.iacademic.info/nxtb/EN/10.11924/j.issn.1000-6850.casb2020-0426 (accessed on 14 June 2021).
12. Li K, Zhao S, Guan W, Li KJ. Planktonic bacteria in white shrimp (*Litopenaeus vannamei*) and channel catfish (*Letalurus punetaus*) aquaculture ponds in a salt-alkaline region. *Lett. Appl. Microbiol.* **2022**, *74*, 212–219. DOI:10.1111/lam.13600
13. Weirich CR, Tiersch TR. Effects of Environmental Sodium Chloride on Percent Hatch, Yolk Utilization, and Survival of Channel Catfish Fry. *J. World Aquac. Soc.* **1997**, *28*, 289–296. DOI:10.1111/j.1749-7345.1997.tb00645.x
14. Su B, Perare DA, Mu X, Dunham RA. Effect of sodium chloride on hatching rate on channel catfish, *Ictalurus punctatus*, Embryos. *J. Appl. Aquac.* **2013**, *25*, 283–292. DOI:10.1080/10454438.2013.848754
15. Abass NY, Elwakil HE, Hemeida AA, Abdelsalam NR, Ye Z, Su B, et al. Genotype–environment interactions for survival at low and sub-zero temperatures at varying salinity for channel catfish, hybrid catfish and transgenic channel catfish. *Aquaculture* **2016**, *458*, 140–148. DOI:10.1016/j.aquaculture.2016.02.031
16. Zhang SY, Shao JJ, Chen XH, Wang MH, Zhong LQ, Qin Q, et al. Effects of salinities on growth, water binding capacity and nutrients of in channel catfish fingerlings. *J. Biol.* **2018**, *35*, 57–61. Available online: http://www.swxzz.com/EN/abstract/abstract474.shtml (accessed on 18 June 2018).
17. Duan YQ, Liu HY, Wang MH, Zhong LQ, Su CF, Liu J, et al. Effects of salt stress on growth and tissue enzyme activity of juvenile Channel Catfish (*Ictalurus punctatus*). *Chin. Agric. Sci. Bull.* **2025**, *41*, 143–150. DOI:10.11924/j.issn.1000-6850.casb2024-0481
18. National Health and Family Planning Commission of PRC. *GB 5009.168-2016*; National Food Safety Standard: Determination of Fatty Acids in Food. China Standards Press: Beijing, China, 2016. Available online: https://www.spc.org.cn/online/58ff4b22db251f38a09d741e7520218a.html (accessed on 23 December 2016).
19. National Health and Family Planning Commission of PRC. *GB 5009.268-2016*; National Food Safety Standard: Determination of Multiple Elements in Food. China Standards Press: Beijing, China, 2016. Available online: https://www.spc.org.cn/online/7b57cc9f015bb4486686f217de902eb4.html (accessed on 23 December 2016).

20. Zhang M, Pan D, Jin B, Zheng R, Xuan Y. Development of a certified reference material for accurate determination of the leaching of Pb and Zn in solid waste. *Anal. Bioanal. Chem.* **2023**, *415*, 6355–6362. DOI:10.1007/s00216-023-04912-3
21. Ernst J, Bar-Joseph Z. STEM: A tool for the analysis of short time series gene expression data. *BMC Bioinform.* **2006**, *7*, 191. DOI:10.1186/1471-2105-7-191
22. Zhang H, Zhang X, Zhao X, Xu J, Lin C, Jing P, et al. Discrimination of dried sea cucumber (*Apostichopus japonicus*) products from different geographical origins by sequential windowed acquisition of all theoretical fragment ion mass spectra (SWATH-MS)-based proteomic analysis and chemometrics. *Food Chem.* **2019**, *274*, 592–602. DOI:10.1016/j.foodchem.2018.08.082
23. Zhao G, Zhai X, Qu M, Tong C, Li W. Sulfated modification of the polysaccharides from *Crassostrea gigas* and their antioxidant and hepatoprotective activities through metabolomics analysis. *Int. J. Biol. Macromol.* **2019**, *129*, 386–395. DOI:10.1016/j.ijbiomac.2019.02.053
24. Ashburner M, Ball CA, Blake JA, Botstein D, Butler H, Cherry JM, et al. Gene Ontology: Tool for the unification of biology. *Nat. Genet.* **2000**, *25*, 25–29. DOI:10.1038/75556
25. Kanehisa M. KEGG: Kyoto Encyclopedia of Genes and Genomes. *Nucleic Acids Res.* **2000**, *28*, 27–30. DOI:10.1093/nar/28.1.27
26. Benjamini Y, Hochberg Y. Controlling the False Discovery Rate: A Practical and Powerful Approach to Multiple Testing. *J. R. Stat. Soc. Ser. B: Stat. Methodol.* **1995**, *57*, 289–300. DOI:10.1111/j.2517-6161.1995.tb02031.x
27. Bouhaddani SE, Houwing-Duistermaat J, Salo P, Perola M, Jongbloed G, Uh HW. Evaluation of O2PLS in Omics data integration. *BMC Bioinform.* **2016**, *17*, 117–132. DOI:10.1186/s12859-015-0854-z
28. Deane EE, Woo NYS. Modulation of fish growth hormone levels by salinity, temperature, pollutants and aquaculture related stress: A review. *Rev. Fish. Biol. Fish.* **2009**, *19*, 97–120. DOI:10.1007/s11160-008-9091-0
29. Sun S, Gong C, Deng C, Yu H, Zheng D, Wang L, et al. Effects of salinity stress on the growth performance, health status, and intestinal microbiota of juvenile *Micropterus salmoides*. *Aquaculture* **2023**, *576*, 739888. DOI:10.1016/j.aquaculture.2023.739888
30. Fang H, Yang YY, Wu XM, Zheng SY, Song YJ, Zhang J, et al. Effects and Molecular Regulation Mechanisms of Salinity Stress on the Health and Disease Resistance of Grass Carp. *Front. Immunol.* **2022**, *13*, 917497. DOI:10.3389/fimmu.2022.917497
31. Zhang L, Liu Z, Deng Y, He C, Liu W, Li X. The Benefits of Nanosized Magnesium Oxide in Fish *Megalobrama amblycephala*: Evidence in Growth Performance, Redox Defense, Glucose Metabolism, and Magnesium Homeostasis. *Antioxidants* **2023**, *12*, 1350. DOI:10.3390/antiox12071350
32. Bhatt S, Dasgupta S, Gupta S, Sahu NP, Kumar VJR, Varghese T. Effect of sulfate on the osmoregulatory and physio-biochemical responses of GIFT (*Oreochromis niloticus*) juveniles reared in potassium-deficient medium saline waters. *Environ. Sci. Pollut. Res.* **2024**, *31*, 18636–18655. DOI:10.1007/s11356-024-32219-y
33. Kong Y, Wei S, Ding Z, Qi C, Liu Y, Zhang Y, et al. Dietary magnesium improves the growth, antioxidant capacity, ammonia nitrogen tolerance and intestinal health of juvenile oriental river prawn *Macrobrachium nipponense*. *Aquaculture* **2022**, *560*, 738557. DOI:10.1016/j.aquaculture.2022.738557
34. Zhang S, Duan Y, Zhong L, Liu H, Wang M, Chen X. Using comparative transcriptome analysis to identify molecular response mechanisms to salinity stress in channel catfish (*Ictalurus punctatus*). *Environ. Pollut.* **2023**, *333*, 121911. DOI:10.1016/j.envpol.2023.121911
35. Saffari S, Keyvanshokooh S, Zakeri M, Johari SA, Pasha-Zanoosi H. Effects of different dietary selenium sources (sodium selenite, selenomethionine and nanoselenium) on growth performance, muscle composition, blood enzymes and antioxidant status of common carp (*Cyprinus carpio*). *Aquacult Nutr.* **2017**, *23*, 611–617. DOI:10.1111/anu.12428
36. Hao JY, Lin Y, Pan WJ, Jiang WQ, Liu B, Miao LH, et al. Dietary selenium enhances the growth and anti-oxidant capacity of juvenile blunt snout bream (*Megalobrama amblycephala*). *Fish. Shellfish. Immunol.* **2020**, *101*, 115–125. DOI:10.1016/j.fsi.2020.03.041
37. Hoo Fung LA, Antoine JMR, Grant CN, Buddo DSA. Evaluation of dietary exposure to minerals, trace elements and heavy metals from the muscle tissue of the lionfish *Pterois volitans* (Linnaeus 1758). *Food Chem. Toxicol.* **2013**, *60*, 205–212. DOI:10.1016/j.fct.2013.07.044
38. Péron M, Gonzalvez R, Hue S, Soudant P, Le Grand F, Mazurais D, et al. Spatial and ontogenetic modulation of fatty acid composition in juvenile European sea bass (*Dicentrarchus labrax*) from two French estuaries. *Mar. Environ. Res.* **2024**, *197*, 106456. DOI:10.1016/j.marenvres.2024.106456
39. Tsoupras A, Brummell C, Kealy C, Vitkaitis K, Redfern S, Zabetakis I. Cardio-Protective Properties and Health Benefits of Fish Lipid Bioactives; The Effects of Thermal Processing. *Mar. Drugs* **2022**, *20*, 187. DOI:10.3390/md20030187

40. Cui J, Cao J, Ge J, Qu X, Li P, Li C. Comprehensive lipid profiles of sea cage aquaculture cobia (*Rachycentron canadum*) based on lipidomics. *J. Food Compos. Anal.* **2022**, *112*, 104664. DOI:10.1016/j.jfca.2022.104664
41. Cui J, Jiang X, Zhang W, Li C, Cao J. Positional characterization of DHA/EPA in triacylglycerol and phospholipid and production of DHA/EPA-rich phospholipid. *J. Food Compos. Anal.* **2024**, *129*, 106085. DOI:10.1016/j.jfca.2024.106085
42. Marques VH, Moreira RG, Branco GS, Honji RM, Rombenso AN, Viana MT, et al. Different saturated and monounsaturated fatty acids levels in fish oil-free diets to cobia (*Rachycentron canadum*) juveniles: Effects in growth performance and lipid metabolism. *Aquaculture* **2021**, *541*, 736843. DOI:10.1016/j.aquaculture.2021.736843
43. Lu Y, Zhang P, Li W, Liu J, Shang X, Cheng Y, et al. Comparison of gut microbial communities, free amino acids or fatty acids contents in the muscle of wild *Aristichthys nobilis* from Xinlicheng reservoir and Chagan lake. *BMC Microbiol.* **2022**, *22*, s12866. DOI:10.1186/s12866-022-02440-1
44. Pekkoeva SN, Voronin VP, Falk-Petersen S, Berge J, Nemova NN, Murzina SA. Fatty Acids Composition of the Muscles of *Leptoclinus maculatus* (Stichaeidae) postlarvae from Kongsfjord and Rijpfjord, Spitsbergen. *J. Ichthyol.* **2022**, *62*, 987–996. DOI:10.1134/S0032945222050113
45. Tang L, Duan Y, Xie B, Liu H, Zhong L, Wang M, et al. Effects of salinity stress on the growth performance, histological characteristics, and expression of genes related to apoptosis and immunity in channel catfish (*Ictalurus punctatus*). *J. Fish. Biol.* **2025**, *106*, 1112–1123. DOI:10.1111/jfb.16029
46. Zhang T, Zhang L, Yin T, You J, Liu R, Huang Q, et al. Recent understanding of stress response on muscle quality of fish: From the perspective of industrial chain. *Trends Food Sci. Technol.* **2023**, *140*, 104145. DOI:10.1016/j.tifs.2023.104145
47. El-Leithy AAA, Hemeda SA, El Naby WSHA, El Nahas AF, Hassan SAH, Awad ST, et al. Optimum salinity for Nile tilapia (*Oreochromis niloticus*) growth and mRNA transcripts of ion-regulation, inflammatory, stress- and immune-related genes. *Fish. Physiol. Biochem.* **2019**, *45*, 1217–1232. DOI:10.1007/s10695-019-00640-7
48. Mohamed NA, Saad MF, Shukry M, El-Keredy AMS, Nasif O, Van Doan H, et al. Physiological and ion changes of Nile tilapia (*Oreochromis niloticus*) under the effect of salinity stress. *Aquac. Rep.* **2021**, *19*, 100567. DOI:10.1016/j.aqrep.2020.100567